ACS APPLIED MATERIALS & INTERFACES

Research Article

www.acsami.org

Semitransparent Fully Air Processed Perovskite Solar Cells

Lingling Bu, Zonghao Liu, Meng Zhang, Wenhui Li, Aili Zhu, Fensha Cai, Zhixin Zhao,* and Yinhua Zhou*

Wuhan National Laboratory for Optoelectronics, Huazhong University of Science and Technology, Wuhan 430074, China

Supporting Information

ABSTRACT: Semitransparent solar cells are highly attractive for application as power-generating windows. In this work, we present semitransparent perovskite solar cells that employ conducting polymer poly(3,4-ethylenedioxythiophene):poly(styrenesulfonate) (PEDOT:PSS) film as the transparent counter electrode. The PEDOT:PSS electrode is prepared by transfer lamination technique using plastic wrap as the transfer medium. The use of the transfer lamination technique avoids the damage of the $CH_3NH_3PbI_3$ perovskite film by direct contact of PEDOT:PSS aqueous solution. The semitransparent perovskite solar cells yield a power conversion efficiency of 10.1% at an area of about 0.06 cm^2 and 2.9% at an area of 1 cm^2. The device structure and the fabrication technique provide a facile way to produce semitransparent perovskite solar cells.

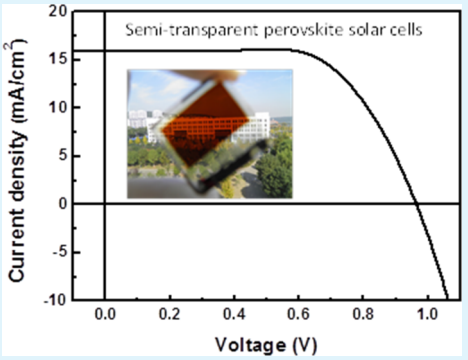

KEYWORDS: *perovskite solar cell, semitransparent, PEDOT:PSS counter electrode, plastic wrap, transfer lamination technique, large-area proviskite solar cell*

1. INTRODUCTION

Low-cost and easily processed semitransparent solar cells are highly attractive for application as power-generating windows. In the past, semitransparent solar cells have been demonstrated based on organic bulk-heterojunction active layers because of their easily tunable bandgap and the easy processing of the organic active layer.[1−11] So far, the reported efficiency of optimized organic semitransparent solar cells is about 5−7%.[11−13] The efficiency is limited by the use of the organic active layer because the optimized single-junction organic solar cells exhibit a highest efficiency of 10−11%. Recently, organic−inorganic lead halide perovskite ($CH_3NH_3PbX_3$)-based thin film photovoltaic devices have been attracting great attention owing to their high efficiency and easy processing. As a new absorber, the perovskite materials own special properties such as large light absorption coefficient,[14] high carrier mobility,[15,16] direct band gap,[17] and long carrier diffusion length.[18,19] The efficiency of the perovskite solar cells has been enhanced very rapidly in the past three years, and the present record high efficiency has reached 20.1%.[20−25] The high efficiency of the perovskite absorbers-based solar cells provides the possibility to fabricate more efficient semitransparent solar cells than those based on organic active layers.

To fabricate semitransparent solar cells, both electron- and hole-collecting electrodes must be transparent. The following transparent conductive materials have been used as transparent electrodes, including transparent conducting oxides (TCO), conducting polymer, silver nanowire,[26,27] and graphene.[28] Transparent conducting oxides (TCO) such as indium−tin oxides (ITO) or fluorine-doped tin oxides (FTO) are typically used as the bottom electrodes in perovskite solar cells. Transparent electrode materials such as carbon nanotube,[29] thin Au or Au/Li film,[30,31] multilayered dielectric-metal-dielectric structure,[32] Ag nanowire,[33] and nickel mesh[34] were applied to fabricate the semitransparent perovskite solar cells. As for the transparent top electrode conducting polymer poly(3,4-ethylenedioxythiophene): poly(styrenesulfonate) (PEDOT:PSS) could be a good candidate because of the easy fabrication (solution processing), high transmittance (over 90% at 100 nm), and high conductivity (over 1000 S/cm).[35−37] PEDOT:PSS thin films have been widely used in organic solar cells,[36−39] antistatic coatings,[40] organic light emitting diodes,[41] supercapacitors,[25] and organic thin film transistors.[42] The PEDOT and PSS are ionically bound and dispersed in water. Since the active layer of organic−inorganic lead halide perovskite ($CH_3NH_3PbX_3$) is sensitive to humidity, direct coating of the PEDOT:PSS aqueous solution on top of the perovskite layer would directly convert the $CH_3NH_3PbX_3$ into PbI_2. The color changes from dark brown into yellow. To solve the incompatibility of humidity-sensitive perovskite film and the PEDOT:PSS film processing, a film-transfer lamination technique is an appropriate method to prepare the perovskite film, where the PEDOT:PSS film is first deposited on a transfer medium (such as polydimethylsiloxane) and then transfer-laminated onto the receiving surface.[43] The PEDOT:PSS film is transferred on top of the perovskite film in dry and will not damage the perovskite film.

Received: May 10, 2015
Accepted: July 21, 2015
Published: July 21, 2015

DOI: 10.1021/acsami.5b04040
ACS Appl. Mater. Interfaces 2015, 7, 17776−17781

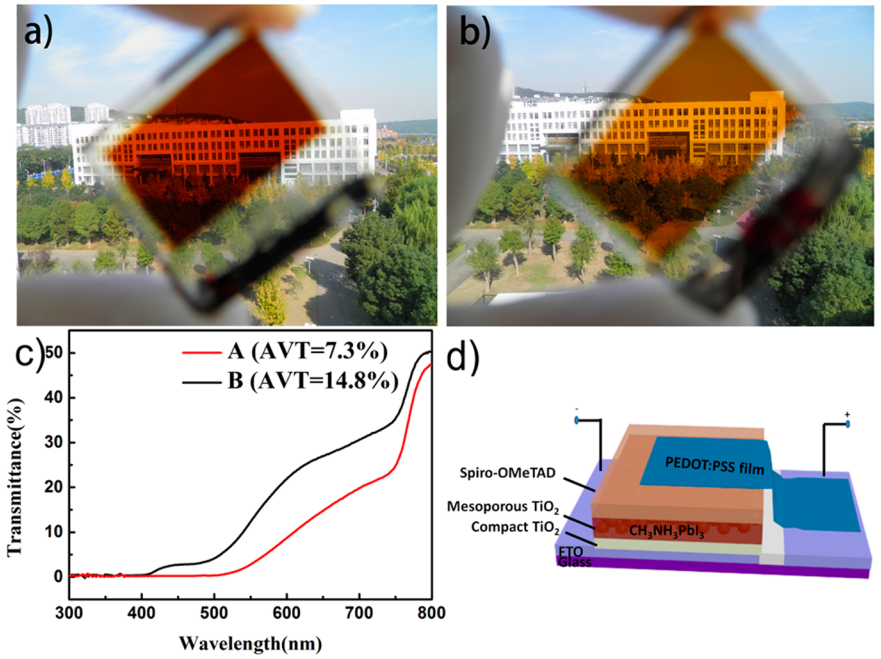

Figure 1. Pictures of the semitransparent perovskite devices (FTO/c-TiO_2/m-TiO_2/$CH_3NH_3PbI_3$/HTM/PEDOT:PSS): (a) the cell with 240 nm m-TiO_2 thickness (cell A); (b) the cell with 140 nm m-TiO_2 (cell B); (c) transmittance of the two semitransparent solar cells; (d) device structure of $CH_3NH_3PbI_3$ perovskite solar cells.

In this work, we demonstrate semitransparent perovskite using FTO as the bottom electrode and PEDOT:PSS as the top electrode. Both the electrodes are transparent, and the semitransparent cells are metal-free. The PEDOT:PSS electrode is prepared on top of the perovskite layers via a transfer lamination technique with plastic wrap as the transfer medium. Transmittance (T) of the fabricated solar cells is tuned by changing the thickness of the TiO_2 scaffold layer and the concentration of the PbI_2 solution. The semitransparent cells exhibit a power conversion efficiency (PCE) of 10.1% under AM1.5 global 1 sun solar illumination when the device area is 0.06 cm^2 and 2.9% when the device area is 1 cm^2 with an average visible transmittance (AVT) of 7.3%.

2. EXPERIMENTAL SECTION

2.1. Materials. Unless otherwise stated, all of materials were purchased from Sigma-Aldrich. Spiro-OMeTAD was purchased from Luminescence Technology Corp. 2-Propanol (Aladdin) was used in the process of transfer of the PEDOT:PSS film. CH_3NH_3I was synthesized according to the reported procedure.[44] 5 wt % ethylene glycol (Aladdin) was added into PEDOT:PSS PH1000 (Heraeus) to enhance its conductivity, and 0.5 wt % Superwet-340 (Tianjin SurfyChem T&D Co.) was dispersed in the PH1000 solution to tune the wetting property on the plastic wrap (polymethylpentene, PMP, Miaojie) medium.

2.2. Solar cell fabrication. First, a 20 nm-thick TiO_2 compact layer (c-TiO_2) was coated on the cleaned FTO substrates by aerosol spray pyrolytic deposition of a titanium diisopropoxide bis(acetylacetonate) solution. A mesoporous TiO_2 (m-TiO_2) layer was deposited by spin coating at 6,000 r.p.m. for 30 s using a TiO_2 paste (Dyesol 18NRT) diluted in ethanol (1:4 and 1:8, w/w, respectively). Then the TiO_2 films were gradually heated to 500 °C, baked at this temperature for 30 min, and cooled to room temperature. PbI_2 was dissolved in *N*,*N*-dimethylformamide at a concentration of 462 mg mL^{-1} (1 M) and 231 mg mL^{-1} (0.5 M), spin-coated at 6,500 r.p.m. for 90 s, and dried at 70 °C for 30 min. Then, the films were dipped in a solution of CH_3NH_3I in 2-propanol (10 mg mL^{-1}) for 60 s, rinsed with 2-propanol, and dried at 70 °C for 30 min.[45] The hole transporting layer was then deposited by spin coating at 4,000 r.p.m. for 30 s from a solution of 72.3 mg of spiro-OMeTAD, 17.5 μL of a stock solution of 520 mg mL^{-1} lithium bis(trifluoromethylsulfonyl)-imide in acetonitrile, and 29 μL of 4-*tert*-butylpyridine in 1 mL of chlorobenzene. Finally, the PEDOT:PSS film was transfer-laminated as the top electrode. The transfer lamination procedure of the PEDOT:PSS film was prepared according to our previous paper.[46] The transfer process of the PH1000 film and the schematic of the finished device are shown in Figure S1. In brief, plastic wrap films were adhered onto glass substrates by adding ethanol in between. PEDOT:PSS (Clevios PH 1000) solution with 5 wt % ethylene glycol and 0.5 wt % surfactant was spin-coated onto the plastic wrap at 500 r.p.m. for 18 s and dried in air. One drop of 2-propanol was dropped onto the PH1000 film on plastic wrap to release the adhesion between PEDOT:PSS film, plastic wrap, and the glass substrate, so that they can separate from each other. The plastic wrap with PEDOT:PSS film was transferred onto the receiving surface of FTO/c-TiO_2 layer/m-TiO_2/$CH_3NH_3PbI_3$/spiro-OMeTAD. Then the plastic wrap was peeled off before the 2-propanol was evaporated to finish the transfer lamination of PH1000. The thickness of PH1000 is about 175 nm. Electrical wires were soldered onto the FTO and PH1000 electrodes outside of the effective device area to make good contact for measurement as shown in Figure 1d. Solar cells with small device area (about 6 mm^2) and large area (2.4 cm^2) were both fabricated.

2.3. Film and device characterization. The irradiance of 100 mW cm^{-2} was offered by a xenon light source solar simulator (#9119, Newport) with an AM 1.5G filter (#91192, Newport). The current density−voltage (J−V) characteristics of the devices under these conditions were obtained by applying external potential bias to the devices, and the generated photocurrent was measured with a Keithley model 2400 digital source meter. For the small area cell (6 mm^2), no aperture was used during the measurement. The device area is determined by the overlap of the FTO bottom electrode and top PH1000 electrode. For the large area, apertures with different area were used during the measurement to investigate the effect of aperture area on the device performance. Incident photon-to-current conversion efficiency (IPCE) spectra were measured using a white light bias and with AC model (10 Hz), and the acquisition system (#70714, Newport) was similar to the J−V test system. The devices were tested in a dark environment to prevent light scattering. The

DOI: 10.1021/acsami.5b04040
ACS Appl. Mater. Interfaces 2015, 7, 17776−17781

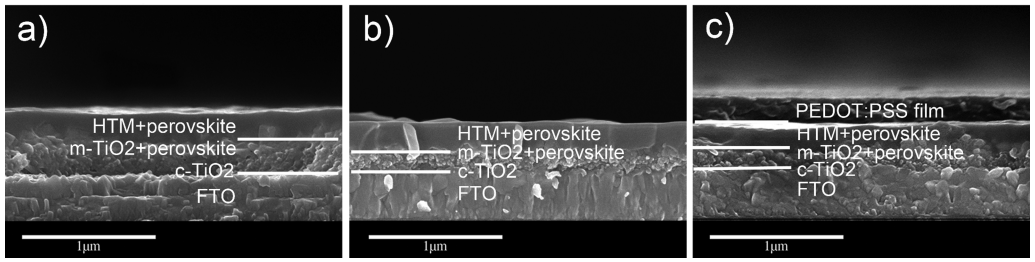

Figure 2. Cross-sectional images: (a) FTO/c-TiO_2/m-TiO_2 (*240 nm*)/perovskite/HTM; (b) FTO/c-TiO_2/m-TiO_2 (*140 nm*)/perovskite/HTM; (c) FTO/c-TiO_2/m-TiO_2 (*140 nm*)/perovskite/HTM/PEDOT:PSS film.

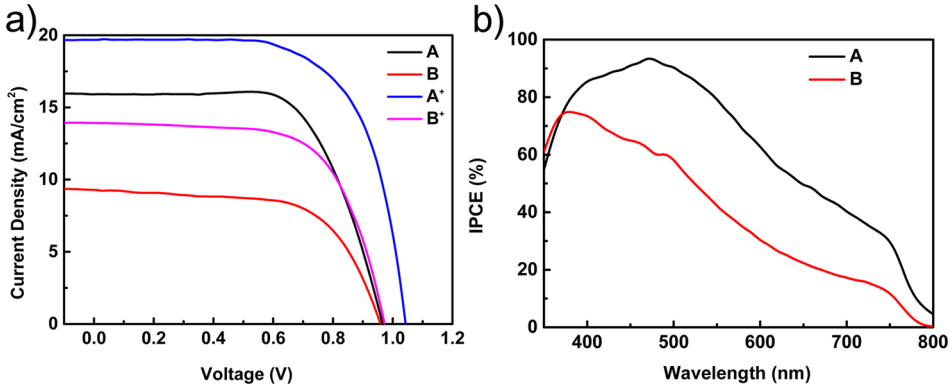

Figure 3. (a) *J*−*V* characteristic of the cells (small area: 6 mm^2) measured under AM1.5G 100 mW cm^{-2} illumination: with 240 nm m-TiO_2 (cell A, A^+) and with 140 nm m-TiO_2 (B, B^+). A and B denote the semitransparent cells with transfer-laminated PEDOT:PSS top electrodes, while A^+ and B^+ denote the reference cells with thermally deposited Au top electrode. (b) IPCE spectra of the two semitransparent solar cells.

transmittance spectra of the devices were measured by using PerkinElmer Lambda 950 (P/N-L6020036). The images of the cross section of cells were taken using Nova Nano SEM 450 (FEI Company).

3. RESULTS AND DISCUSSION

Figure S2a shows the transmittance and sheet resistance of PEDOT:PSS films by spin coating and transfer lamination. The two films exhibit similar transmittance and sheet resistance of about 85 ohm/sq. The thickness of the PH1000 films is about 175 nm, and therefore, the conductivity of the PH1000 films is calculated to be about 670 S/cm. Figure 1a and 1b are pictures of two perovskite solar cells with area of 1.2 cm × 2.0 cm on 2.5 cm × 2.5 cm FTO-covered glass substrates with different transmittances. The transmittance of the semitransparent cells was tuned by changing the thickness of the m-TiO_2 scaffold layer and the concentration of the PbI_2 solution. In Figure 1a, a picture of the fabricated semitransparent cell with a 240 nm m-TiO_2 layer is shown, placed with the outside scenery as the background to demonstrate the transparency. The white buildings and trees outside can be clearly seen through the brown cell. In Figure 1b, the picture presents the light brown color with a thinner 140 nm m-TiO_2 layer, which is more transparent than the thick one. Figure 1c shows the transmittance of the two cells. The transmittance values of the thick device and the thin device are 2.7% and 12.3% at 550 nm. The thicker cell (with 240 nm m-TiO_2) shows an AVT of 7.3% and the thinner cell (with 140 nm m-TiO_2) shows an AVT of 14.8% in the spectral range of 370−740 nm.

The schematic of the $CH_3NH_3PbI_3$ perovskite solar cells with the PEDOT:PSS film as the top electrode is shown in Figure 1d. The working mechanism is similar to that of the typical gold electrode perovskite solar cell. $CH_3NH_3PbI_3$ nanocrystalline infiltrated the n-type m-TiO_2, and the hole transporting material (HTM) is deposited on top of the perovskite film. The incident light illuminates through the glass, and charge carriers are generated in the $CH_3NH_3PbI_3$ absorber layer. The electrons are collected by the TiO_2, and the holes are collected by the Spiro-OMeTAD layer and PEDOT:PSS counter electrode.[17,47]

Figure 2 shows cross-sectional scanning electron microscopy (SEM) images of the layers before and after PEDOT:PSS film deposition. Figure 2a and 2b show the layers FTO/c-TiO_2/m-TiO_2/perovskite/HTM before PEDOT:PSS deposition where the m-TiO_2 layer is 240 nm (Figure 2a) and 140 nm (Figure 2b), respectively. Figure 2c shows the cross-section of the whole cell with the PEDOT:PSS top electrode. The thickness of the m-TiO_2 layer in Figure 2c is 140 nm, which is the same as that in Figure 2b. The layer of the PEDOT:PSS film can be clearly recognized, and its thickness is about 180 nm.

To evaluate the efficiency of the semitransparent cells with the device structure in Figure 1d, we first fabricated the cells in a small area of 0.06 cm^2. Figure 3 shows the *J*−*V* characteristics and external quantum efficiency of both thicker (240 nm m-TiO_2) and thinner (140 nm m-TiO_2) cells. For the cell with thicker m-TiO_2 (240 nm, cell A), the cell exhibited a V_{OC} of 0.966 V, a J_{SC} of 16.0 mA cm^{-2}, and a fill factor of 65.4, yielding a PCE of 10.1% under AM1.5 100 mW cm^{-2} illumination. For the cell with thinner m-TiO_2 (140 nm, cell B), a lower PCE of 5.6% is achieved with a V_{OC} of 0.959 V, a J_{SC} of 9.2 mA cm^{-2}, and a fill factor of 63.3. The main difference is the J_{SC}, which is associated with the thickness of the perovskite absorber layer. It should be mentioned that the semitransparent cells are fully processed in air. Photovoltaic data of six independent cells are summarized in Tables S1 (cell A) and S2 (cell B). Figure S2 shows the *J*−*V* characteristics of the semitransparent at

DOI: 10.1021/acsami.5b04040
ACS Appl. Mater. Interfaces 2015, 7, 17776−17781

different scan directions to check the hysteresis in these cells. The photovoltaic parameters of cells have been presented in Table S3. The thick device exhibits V_{OC} = 1.0 V, J_{SC} = 15.1 mA/cm^2, FF = 64.3, and PCE = 9.8% while sweeping direction from Forward to Reverse, and the photovoltaic parameters were V_{OC} = 1.0 V, J_{SC} = 15.4 mA/cm^2, FF = 60, and PCE = 8.8% in the inverse scan direction. The thin device exhibits V_{OC} = 0.93 V, J_{SC} = 9.9 mA/cm^2, FF = 61.3, and PCE = 5.6% while sweeping from Forward to Reverse, and V_{OC} = 0.94 V, J_{SC} = 9.8 mA/cm^2, FF = 55.8, and PCE = 5.1% while sweeping from Reverse to Forward. In addition, to obtain reliable device efficiency of the semitransparent perovskite solar cells, we measured the stabilized photocurrent density of the device A and B held at a bias of 0.64 and 0.56 V near their maximum output power point as a function of time to confirm their efficiency, while the photocurrent density of device A is 13.1 mA/cm^2, with a PCE of 8.4%, and that of device B is 8.39 mA/cm^2, with a PCE of 4.7% (Figure S4). For comparison, the reference cells with Au top electrode were also fabricated where the Au electrode is thermally deposited (FTO/c-TiO_2/m-TiO_2/$CH_3NH_3PbI_3$/spiro-OMeTAD/Au). The reference solar cells present a higher PCE of 13.4% and 8.9% for the thicker (cell A$^+$) and thinner (cell B$^+$) cells (Table 1). The higher PCE is mainly ascribed to the higher J_{SC} than semitransparent PEDOT:PSS cells because of the Au electrode also acting as a light reflector, resulting in a higher J_{SC}. Figure 3b reveals the IPCE spectra of the thick device (cell A). The higher semitransparent thin cell (cell B) shows the same trend. The absence of metal electrode as the light reflector in the semitransparent cells results in lower IPCE in the spectral region of 500−800 nm, leading to the lower J_{SC} than that of reference cells with a Au electrode.

Table 1. Photovoltaic Performance of the Solar Cells (device area: 0.06 cm^2): with 240 nm m-TiO_2 (cell A, A$^+$) and with 140 nm m-TiO_2 (B, B$^+$)[a]

Device: Thickness of m-TiO_2, top electrode	V_{OC} (V)	J_{SC} (mA cm^{-2})	FF (%)	PCE (%)
A: 240 nm m-TiO_2, PEDOT:PSS	0.966	16.0	65.4	10.1
A$^+$: 240 nm m-TiO_2, Au	1.045	19.7	64.9	13.4
B: 140 nm m-TiO_2, PEDOT:PSS	0.959	9.2	63.3	5.6
B$^+$: 140 nm m-TiO_2, Au	0.970	13.9	65.7	8.9

[a]A and B denote the semitransparent cells with transfer-laminated PEDOT:PSS top electrodes, while A$^+$ and B$^+$ denote the reference cells with thermally-deposited Au top electrode.

Plastic wrap film as transfer medium has the advantage of large area with low cost. With this merit, here we demonstrate semitransparent solar cells with a large area of about 2.4 cm^2 (shown in Figure 1a and 1b). Seven different areas of masks were used to measure the photovoltaic performance of the semitransparent solar cells, and the definition of aperture area differs from that of a small area cell: the small cell was controlled by the size of the PEDOT:PSS film. Table 2 respectively reveals the values of V_{OC}, J_{SC}, FF, and PCE measured with a representative thick device (type A) and thin device (type B) using masks of different aperture areas, under AM 1.5 100 mW cm^{-2} illumination. Figure 4 shows the photovoltaic parameters (V_{OC}, J_{SC}, FF, and PCE) as a function of aperture area. For cells A, the V_{OC} is 0.941 V when the aperture area is 1 cm × 1 cm. When the aperture area decreases, the V_{OC} drops, and it drops down to 0.841 V when the device area is 0.16 cm^2. For cell B, the V_{OC} follows a similar trend (Figure 4a). This can be explained by the following equation:

Table 2. Photovoltaic Parameters of Large-Area (2.4 cm^2) Semi-transparent Solar Cells (Cell A: with 240 nm m-TiO_2, Cell B: 140 nm m-TiO_2) Measured with Different Aperture Area under Simulated AM 1.5 (100 mW cm^{-2})

Device	Aperture area (cm^2)	V_{OC} (V)	J_{SC} (mA cm^{-2})	FF (%)	PCE (%)
A	1	0.941	11.4	27.3	2.9
	0.8	0.913	12.2	29.8	3.3
	0.6	0.901	13	33.6	3.9
	0.5	0.89	13.5	35.2	4.2
	0.4	0.882	13.8	39	4.7
	0.25	0.86	14.6	45.2	5.7
	0.16	0.841	15.6	50.6	6.7
B	1	0.836	6.1	34.4	1.8
	0.8	0.825	6.4	36.6	1.9
	0.6	0.808	6.5	40.6	2.1
	0.5	0.799	6.9	41.3	2.3
	0.4	0.791	7.3	42.7	2.5
	0.25	0.776	8.3	45.5	2.9
	0.16	0.758	9.3	48.6	3.4

$$V_{OC} = n\frac{kT}{e}\ln\left\{1 + \frac{I_{SC}}{I_0}\right\} \quad (1)$$

where n is the diode ideality factor, k is Boltzmann's constant, T is the absolute temperature, and I_0 is the reverse saturation current. $I_{SC}/I_0 \gg 1$. From eq 1, V_{OC} is expected to be linearly dependent on the $\ln(I_{SC})$, where I_{SC} is determined by the aperture area, which is consistent with what we observed. Figure 4b and 4c reveals that the J_{SC} and FF values of cell A and B decrease with the increase of the aperture area. The J_{SC} and FF both drop when the aperture area increases. The drop of J_{SC} is probably because more defects exist in a larger area. The drop in FF is mainly associated with the increased normalized series resistance ($r_s = R_s/R_{ch}$ with $R_{ch} = V_{oc}/I_{sc}$).[48] The well-working large-area cells A and B indicate that the transfer lamination technique with low cost plastic wrap as the transfer medium is promising for low-cost semitransparent perovskite solar cells.

4. CONCLUSIONS

We have presented that the PEDOT:PSS conductive polymer electrodes can be transferred on top of the perovskite layer using low-cost plastic wrap medium and therefore demonstrated semitransparent perovskite solar cells. The semitransparent perovskite solar cells are fully processed in air. The cells exhibit a power conversion efficiency of 10.1% in a small area (0.06 cm^2) under 100 mW cm^{-2} AM1.5 illumination when the *AVT* of the perovskite cell is about 7.3% in 370−740 nm. Furthermore, we have also fabricated large-area PEDOT:PSS electrodes with the transfer lamination technique using the plastic wrap as the transfer medium. The large area perovskite cells exhibit a power conversion efficiency of 2.9% and can be further enhanced by depositing a metal grid to reduce the series resistance. The transfer-laminated PEDOT:PSS top electrode provides a low-cost fabrication of organic−inorganic lead halide perovskite solar cells replacing expensive Au electrodes and enables the facile fabrication of the semitransparent perovskite solar cell for power-generating windows application.

DOI: 10.1021/acsami.5b04040
ACS Appl. Mater. Interfaces 2015, 7, 17776−17781

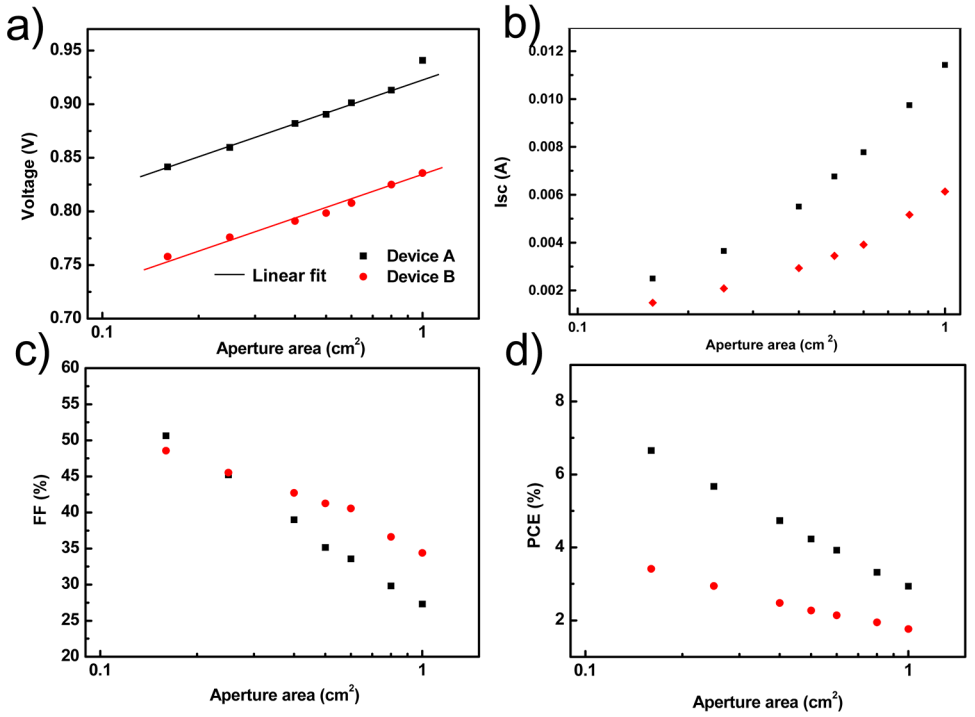

Figure 4. Photovoltaic parameters: (a) V_{OC}, (b) I_{SC}, (c) FF, and (d) PCE of large-area (2.4 cm^2) semitransparent solar cells (cell A: with 240 nm m-TiO_2, cell B: 140 nm m-TiO_2) measured with different aperture areas under simulated AM 1.5 (100 mW cm^{-2}).

■ ASSOCIATED CONTENT

Supporting Information

The Supporting Information is available free of charge on the ACS Publications website at DOI: 10.1021/acsami.5b04040.

J−*V* characteristics of the cells measured with different scanning directions, *I*−*V* characteristics of large-area devices measured using aperture at different device areas, and transfer lamination process of the PEDOT:PSS film and the stabilized current at V_{max} (PDF)

■ AUTHOR INFORMATION

Corresponding Authors

*E-mail: zhixin-zhao@hust.edu.cn (Z.Z.).
*E-mail: yh_zhou@hust.edu.cn (Y.H.Z.).

Notes

The authors declare no competing financial interest.

■ ACKNOWLEDGMENTS

This work was partially supported by the National Basic Research Program of China (973 program 2011CBA00703) and the Fundamental Research Funds for the Central Universities (grant no. HUST: 2014TS016) (Z.Z.). Y.H.Z. acknowledges the support by the Recruitment Program of Global Youth Experts and the National Natural Science Foundation of China (Grant No. 51403071).

■ REFERENCES

(1) Ng, G.-M.; Kietzke, E. L.; Kietzke, T.; Tan, L.-W.; Liew, P.-K.; Zhu, F. Optical Enhancement in Semitransparent Polymer Photovoltaic Cells. *Appl. Phys. Lett.* **2007**, *90*, 103505.

(2) Chen, F.-C.; Wu, J.-L.; Hsieh, K.-H.; Chen, W.-C.; Lee, S.-W. Polymer Photovoltaic Devices with Highly Transparent Cathodes. *Org. Electron.* **2008**, *9*, 1132−1135.

(3) Ameri, T.; Dennler, G.; Waldauf, C.; Azimi, H.; Seemann, A.; Forberich, K.; Hauch, J.; Scharber, M.; Hingerl, K.; Brabec, C. J. Fabrication, Optical Modeling, and Color Characterization of Semitransparent Bulk-Heterojunction Organic Solar Cells in an Inverted Structure. *Adv. Funct. Mater.* **2010**, *20*, 1592−1598.

(4) Lunt, R. R.; Bulovic, V. Transparent, Near-Infrared Organic Photovoltaic Solar Cells for Window and Energy-Scavenging Applications. *Appl. Phys. Lett.* **2011**, *98*, 113305.

(5) Lewis, J. E.; Lafalce, E.; Toglia, P.; Jiang, X. Over 30% Transparency Large Area Inverted Organic Solar Array by Spray. *Sol. Energy Mater. Sol. Cells* **2011**, *95*, 2816−2822.

(6) Colsmann, A.; Reinhard, M.; Kwon, T.-H.; Kayser, C.; Nickel, F.; Czolk, J.; Lemmer, U.; Clark, N.; Jasieniak, J.; Holmes, A. B.; Jones, D. Inverted Semi-Transparent Organic Solar Cells with Spray Coated, Surfactant Free Polymer Top-Electrodes. *Sol. Energy Mater. Sol. Cells* **2012**, *98*, 118−123.

(7) Chen, C.-C.; Dou, L.; Zhu, R.; Chung, C.-H.; Song, T.-B.; Zheng, Y. B.; Hawks, S.; Li, G.; Weiss, P. S.; Yang, Y. Visibly Transparent Polymer Solar Cells Produced by Solution Processing. *ACS Nano* **2012**, *6*, 7185−7190.

(8) Kim, H. P.; Lee, H. J.; Yusoff, A. R. b. M.; Jang, J. Semi-Transparent Organic Inverted Photovoltaic Cells with Solution Processed Top Electrode. *Sol. Energy Mater. Sol. Cells* **2013**, *108*, 38−43.

(9) Kang, Y.-J.; Kim, D.-G.; Kim, J.-K.; Jin, W.-Y.; Kang, J.-W. Progress Towards Fully Spray-Coated Semitransparent Inverted Organic Solar Cells with a Silver Nanowire Eectrode. *Org. Electron.* **2014**, *15*, 2173−2177.

(10) http://www.heliatek.com/ (accessed in May, 2015).

(11) Yu, W.; Jia, X.; Long, Y.; Shen, L.; Liu, Y.; Guo, W.; Ruan, S. Highly Efficient Semitransparent Polymer Solar Cells with Color Rendering Index Approaching 100 Using One-Dimensional Photonic Crystal. *ACS Appl. Mater. Interfaces* **2015**, *7*, 9920−9928.

(12) Romero-Gomez, P.; Betancur, R.; Martinez-Otero, A.; Elias, X.; Mariano, M.; Romero, B.; Arredondo, B.; Vergaz, R.; Martorell, J. Enhanced Stability in Semi-Transparent PTB7/PC71BM Photovoltaic Cells. *Sol. Energy Mater. Sol. Cells* **2015**, *137*, 44−49.

DOI: 10.1021/acsami.5b04040
ACS Appl. Mater. Interfaces 2015, 7, 17776−17781

(13) Chen, K.-S.; Salinas, J.-F.; Yip, H.-L.; Huo, L.; Hou, J.; Jen, A. K. Y. Semi-Transparent Polymer Solar Cells with 6% PCE, 25% Average Visible Transmittance and A Color Rendering Index Close to 100 for Power Generating Window Applications. *Energy Environ. Sci.* **2012**, *5*, 9551−9557.
(14) Kojima, A.; Ikegami, M.; Teshima, K.; Miyasaka, T. Highly Luminescent Lead Bromide Perovskite Nanoparticles Synthesized with Porous Alumina Media. *Chem. Lett.* **2012**, *41*, 397−399.
(15) Mitzi, D. B. Templating and Structural Engineering in Organic−Inorganic Perovskites. *J. Chem. Soc., Dalton Trans.* **2001**, 1−12.
(16) Brivio, F.; Walker, A. B.; Walsh, A. Structural and Electronic Properties of Hybrid Perovskites for High-Efficiency Thin-Film Photovoltaics from First-Principles. *APL Mater.* **2013**, *1*, 042111.
(17) Kim, H. S.; Lee, C. R.; Im, J. H.; Lee, K. B.; Moehl, T.; Marchioro, A.; Moon, S. J.; Humphry-Baker, R.; Yum, J. H.; Moser, J. E.; Gratzel, M.; Park, N. G. Lead Iodide Perovskite Sensitized All-Solid-State Submicron Thin Film Mesoscopic Solar Cell with Efficiency Exceeding 9%. *Sci. Rep.* **2012**, *2*, 591.
(18) Stranks, S. D.; Eperon, G. E.; Grancini, G.; Menelaou, C.; Alcocer, M. J. P.; Leijtens, T.; Herz, L. M.; Petrozza, A.; Snaith, H. J. Electron-Hole Diffusion Lengths Exceeding 1 Micrometer in an Organometal Trihalide Perovskite Absorber. *Science* **2013**, *342*, 341−344.
(19) Xing, G.; Mathews, N.; Sun, S.; Lim, S. S.; Lam, Y. M.; Grätzel, M.; Mhaisalkar, S.; Sum, T. C. Long-Range Balanced Electron-and Hole-Transport Lengths in Organic-Inorganic CH3NH3PbI3. *Science* **2013**, *342*, 344−347.
(20) Kojima, A.; Teshima, K.; Shirai, Y.; Miyasaka, T. Organometal Halide Perovskites as Visible-Light Sensitizers for Photovoltaic Cells. *J. Am. Chem. Soc.* **2009**, *131*, 6050−6051.
(21) Burschka, J.; Pellet, N.; Moon, S.-J.; Humphry-Baker, R.; Gao, P.; Nazeeruddin, M. K.; Gratzel, M. Sequential Deposition as A Route to High-Performance Perovskite-Sensitized Solar Cells. *Nature* **2013**, *499*, 316−319.
(22) Zhou, H.; Chen, Q.; Li, G.; Luo, S.; Song, T.-b.; Duan, H.-S.; Hong, Z.; You, J.; Liu, Y.; Yang, Y. Interface Engineering of Highly Efficient Perovskite Solar Cells. *Science* **2014**, *345*, 542−546.
(23) You, J.; Hong, Z.; Yang, Y.; Chen, Q.; Cai, M.; Song, T.-B.; Chen, C.-C.; Lu, S.; Liu, Y.; Zhou, H.; Yang, Y. Low-Temperature Solution-Processed Perovskite Solar Cells with High Efficiency and Flexibility. *ACS Nano* **2014**, *8*, 1674−1680.
(24) Hodes, G. Perovskite-Based Solar Cells. *Science* **2013**, *342*, 317−318.
(25) Patra, S.; Munichandraiah, N. Supercapacitor Studies of Electrochemically Deposited PEDOT on Stainless Steel Substrate. *J. Appl. Polym. Sci.* **2007**, *106*, 1160−1171.
(26) Liu, C. H.; Yu, X. Silver Nanowire-Based Transparent, Flexible, and Conductive Thin Film. *Nanoscale Res. Lett.* **2011**, *6*, 75.
(27) Langley, D.; Giusti, G.; Mayousse, C.; Celle, C.; Bellet, D.; Simonato, J. P. Flexible Transparent Conductive Materials Based on Silver Nanowire Networks: A Review. *Nanotechnology* **2013**, *24*, 452001.
(28) Jo, G.; Choe, M.; Lee, S.; Park, W.; Kahng, Y. H.; Lee, T. The Application of Graphene as Electrodes in Electrical and Optical Devices. *Nanotechnology* **2012**, *23*, 112001.
(29) Li, Z.; Kulkarni, S. A.; Boix, P. P.; Shi, E.; Cao, A.; Fu, K.w.; Batabyal, S. K.; Zhang, J.; Xiong, Q.; Wong, L. H.; Mathews, N.; Mhaisalkar, S. G. Laminated Carbon Nanotube Networks for Metal Electrode-Free Efficient Perovskite Solar Cells. *ACS Nano* **2014**, *8*, 6797−6804.
(30) Eperon, G. E.; Burlakov, V. M.; Goriely, G.; Snaith, H. J. Neutral Color Semitransparent Microstructured Perovskite Solar Cells. *ACS Nano* **2014**, *8*, 591−598.
(31) Roldán-Carmona, C.; Malinkiewicz, O.; Betancur, R.; Longo, G.; Momblona, C.; Jaramillo, F.; Camacho, L.; Bolink, H. J. High Efficiency Single-Junction Semitransparent Perovskite Solar Cells. *Energy Environ. Sci.* **2014**, *7*, 2968−2973.
(32) Della Gaspera, E.; Peng, Y.; Hou, Q.; Spicciac, L.; Bacha, U.; Jasieniaka, J. J.; Cheng, Y. B. Ultra-Thin High Efficiency Semi-transparent Perovskite Solar Cells. *Nano Energy* **2015**, *13*, 249−257.
(33) Bailie, C. D.; Christoforo, M. G.; Mailoa, J. P.; Bowring, A. R.; Unger, E. L.; Nguyen, W. H.; Lee, J. B.; Gratzel, M.; Noufi, R.; Buonassisi, T.; Salleoa, A.; McGehee, M. D. Semi-Transparent Perovskite Solar Cells for Tandems with Silicon and CIGS. *Energy Environ. Sci.* **2015**, *8*, 956−963.
(34) Eperon, G. E.; Bryant, D.; Troughton, J.; Stranks, S. D.; Johnston, M. B.; Watson, T.; Worsley, D. A.; Snaith, H. J. Efficient, Semitransparent Neutral-Colored Solar Cells Based on Microstructured Formamidinium Lead Trihalide Perovskite. *J. Phys. Chem. Lett.* **2015**, *6*, 129−138.
(35) Xia, Y.; Sun, K.; Ouyang, J. Solution-Processed Metallic Conducting Polymer Films as Transparent Electrode of Optoelectronic Devices. *Adv. Mater.* **2012**, *24*, 2436−2440.
(36) Kim, N.; Kee, S.; Lee, S. H.; Lee, B. H.; Kahng, Y. H.; Jo, Y.-R.; Kim, B.-J.; Lee, K. Highly Conductive PEDOT:PSS Nanofibrils Induced by Solution-Processed Crystallization. *Adv. Mater.* **2014**, *26*, 2268−2272.
(37) Mengistie, D. A.; Ibrahem, M. A.; Wang, P. C.; Chu, C. W. Highly Conductive PEDOT:PSS Treated with Formic Acid for ITO-Free Polymer Solar Cells. *ACS Appl. Mater. Interfaces* **2014**, *6*, 2292−2299.
(38) Ouyang, B. Y.; Chi, C. W.; Chen, F. C.; Xi, Q. F.; Yang, Y. High-Conductivity Poly (3,4-ethylenedioxythiophene): Poly(styrene sulfonate) Film and Its Application in Polymer Optoelectronic Devices. *Adv. Funct. Mater.* **2005**, *15*, 203−208.
(39) Frohne, H.; Shaheen, S. E.; Brabec, C. J.; Müller, D. C.; Sariciftci, N. S.; Meerholz, K. Influence of the Anodic Work Function on the Performance of Organic Solar Cells. *ChemPhysChem* **2002**, *3*, 795−799.
(40) Jonas, F.; Krafft, W.; Muys, B. Poly(3, 4-ethylenedioxythiophene): Conductive Coatings, Technical Applications and Properties. *Macromol. Symp.* **1995**, *100*, 169−173.
(41) Zhang, D.; Ryu, K.; Liu, X.; Polikarpov, E.; Ly, J.; Tompson, M. E.; Zhou, C. Transparent, Conductive, and Flexible Carbon Nanotube Films and Their Application in Organic Light-Emitting Diodes. *Nano Lett.* **2006**, *6*, 1880−1886.
(42) Halik, M.; Klauk, H.; Zschieschang, U.; Kriem, T.; Schmid, G.; Radlik, W.; Wussow, K. Fully Patterned All-OrganicThin Film Transistors. *Appl. Phys. Lett.* **2002**, *81*, 289−291.
(43) Jiang, F.; Liu, T.; Zeng, S.; Zhao, Q.; Min, X.; Li, Z.; Tong, J.; Meng, W.; Xiong, S.; Zhou, Y. Metal Electrode-Free Perovskite Solar Cells with Transfer-Laminated Conducting Polymer Electrode. *Opt. Express* **2015**, *23*, A83−A91.
(44) Im, J. H.; Lee, C. R.; Lee, J. W.; Park, S. W.; Park, N. G. 6.5% Efficient Perovskite Quantum-Dot-Sensitized Solar Cell. *Nanoscale* **2011**, *3*, 4088−4093.
(45) Burschka, J.; Pellet, N.; Moon, S. J.; Humphry-Baker, R.; Gao, P.; Nazeeruddin, M. K.; Gratzel, M. Sequential Deposition as A Route to High-Performance Perovskite-Sensitized Solar Cells. *Nature* **2013**, *499*, 316−319.
(46) Yin, L.; Zhao, Z.; Jiang, F.; Li, Z.; Xiong, S.; Zhou, Y. PEDOT:PSS Top Electrode Prepared by Transfer Lamination Using Plastic Wrap as the Transfer Medium for Organic Solar Cells. *Org. Electron.* **2014**, *15*, 2593−2598.
(47) Tanaka, K.; Takahashi, T.; Ban, T.; Kondo, T.; Uchida, K.; Miura, N. Comparative Study on the Excitons in Lead-Halide-Based Perovskite-Type Crystals CH3NH3PbBr3 CH3NH3PbI3. *Solid State Commun.* **2003**, *127*, 619−623.
(48) Zhou, Y.; Khan, T. M.; Shim, J. W.; Dindar, A.; Fuentes-Hernandez, C.; Kippelen, B. All-Plastic Solar Cells with a High Photovoltaic Dynamic Range. *J. Mater. Chem. A* **2014**, *2*, 3492−3497.

DOI: 10.1021/acsami.5b04040
ACS Appl. Mater. Interfaces 2015, 7, 17776−17781